

# Mesoscopic two-phase model for describing apparent slip in micro-channel flows

R. Benzi<sup>1</sup>, L. Biferale<sup>1</sup>, M. Sbragaglia<sup>1</sup>, S. Succi<sup>2</sup> and F. Toschi<sup>2,3</sup>

<sup>1</sup> Dipartimento di Fisica and INFN, Università di Tor Vergata,  
via della Ricerca Scientifica 1, 00133, Roma, Italy.

<sup>2</sup> Istituto Applicazioni Calcolo, CNR, Viale del Policlinico 137, 00161 Roma, Italy.

<sup>3</sup> INFN, Via del Paradiso 12, 44100 Ferrara, Italy.

The phenomenon of apparent slip in micro-channel flows is analyzed by means of a two-phase mesoscopic lattice Boltzmann model including non-ideal fluid-fluid and fluid-wall interactions. The weakly-inhomogeneous limit of this model is solved analytically. The present mesoscopic approach permits to access much larger scales than molecular dynamics, and comparable with those attained by continuum methods. However, at variance with the continuum approach, the existence of a gas layer near the wall does not need to be postulated a priori, but emerges naturally from the underlying non-ideal mesoscopic dynamics. It is therefore argued that a mesoscopic Lattice Boltzmann approach with non-ideal fluid-fluid and fluid-wall interactions might achieve an optimal compromise between physical realism and computational efficiency for the study of channel micro-flows.

PACS numbers: 47.55.Dz, 47.55.Kf, 47.11+j, 83.50.Rp, 68.08-p

The microscopic physics underlying fluid/solid interactions is fairly rich and complex, for it depends on specific details of molecular interactions as well as on the micro-geometrical details of the boundary. However, on a macroscopic scale, these details can often be safely ignored by assuming that the net effect of surface interactions is simply to prevent any relative motion between the solid walls and the fluid elements next to them. This is the so-called “no-slip” boundary condition, which forms the basis of mathematical treatments of bounded flows as continuum media [1]. No-slip boundary conditions are extremely successful in describing a huge class of viscous flows. Yet, the evidence is that certain classes of viscous flows *do* slip on the wall. Recent advances in microfluidics experiments [2, 3], as well as numerical investigations [4, 5, 6, 7, 8], have identified the conditions which seem to underlie the validity of the no-slip assumption. Namely: (i) single-phase flow; (ii) wetted surfaces and (iii) low levels of shear rates. Under such conditions, careful experiments have shown that fluid comes to rest within a few molecular diameters from the surface [9, 10, 11, 12]. Conditions (i-iii) are not exhaustive, though. For instance, partial slips of simple (Newtonian) flows, such as alkanes and water, is predicted by an increasing number of experiments [13, 14, 15, 16] and simulations [4, 5, 6, 7, 8] (see [17] for a review on experiments and numerics). Under this state of affairs, there appears to be a great need to provide a convincing, and possibly general, theoretical picture for the onset of slip motion. Among others, an increasingly popular explanation is that the flowing fluid would develop a lighter (less dense) phase and dynamically segregate it in the form of a thin film sticking to the wall [18, 19]. This thin film would then provide a “gliding” surface for the bulk fluid which would slip on it without ever coming in contact with the solid wall. This gives rise to the so-called *apparent slip* phenomenon, that is, the extrapolated bulk flow speed would vanish far-out away from the wall, even though the actual flow

speed in the film does vanish exactly at the wall location. This film-picture is very appealing, but still in great need of theoretical clarification. In particular, the underlying mechanisms of film formation are still under question: are they generic or detail-driven?

In this paper we shall propose that film formation is a *generic* phenomenon, which can be captured by a one-parameter mesoscopic approach, lying in-between the microscopic (atomistic) and macroscopic (continuum) levels. The mesoscopic approach is based on a minimal (lattice) Boltzmann equation, (LBE) [20, 21, 23], including non-ideal interactions [22, 24, 25, 26, 27, 28], which can drive dynamic phase transitions. The only free parameter in the LBE is the strength of these non-ideal (potential energy) interactions. Hopefully, the present mesoscopic approach provides an optimal compromise between the need of including complex physics (phase-transition) not easily captured by a continuum approach, and the need of accessing experimentally relevant space-time scales which are out of reach to microscopic Molecular Dynamics (MD) simulations [4, 6, 7, 8]. In particular, at variance with the macroscopic approach, the gas film does not need to be postulated a-priori, but emerges dynamically from the underlying mesoscopic description, by progressive switching of potential interactions. One major advantage of this formulation is that it allows to develop a simple and straightforward analytical interpretation of the results as well as of the effective slip length arising in the flow. This interpretation is based on the macroscopic limit of the model which can be achieved by a standard Chapman-Enskog expansion.

The lattice Boltzmann model used in this paper to describe multiple phases has been developed in [22]. Since this model is well documented in the literature, here we shall provide only the basic facts behind it. We recall that the model is a minimal discrete version of the Boltzmann

equation, and reads as follows:

$$f_i(\mathbf{x} + \mathbf{c}_i, t + 1) - f_i(\mathbf{x}, t) = -\frac{1}{\tau} \left( f_i(\mathbf{x}, t) - f_i^{(eq)}(\mathbf{x}, t) \right) \quad (1)$$

where  $f_i(\mathbf{x}, t)$  is the probability density function associated to a mesoscopic velocity  $\mathbf{c}_i$  and where  $\tau$  is a mean collision time and  $f_i^{(eq)}(\mathbf{x}, t)$  the equilibrium distribution that corresponds to the Maxwellian distribution in the fully continuum limit. The bulk interparticle interaction is proportional to a free parameter,  $\mathcal{G}_b$ , entering the balance equation for the momentum change:

$$\frac{d(\rho \mathbf{u})}{dt} = \mathbf{F} \equiv \mathcal{G}_b \sum_l w_l \Psi[\rho(\mathbf{x})] \Psi[\rho(\mathbf{x} + \mathbf{c}_l)] \mathbf{c}_l \quad (2)$$

being  $w_l$  the equilibrium weights and  $\Psi$  the potential function which describes the fluid-fluid interaction triggered by density variation. By Taylor expanding eq.(2) one recovers, in the hydrodynamical limit, the equation of motion for a non-ideal fluid with equation of state  $P = c_s^2(\rho - \frac{1}{2}\mathcal{G}_b\Psi^2(\rho))$ ,  $c_s$  being the sound speed velocity. With the choice

$$\Psi(\rho) = 1 - \exp(-\rho/\rho_0)$$

with  $\rho_0 = 1$  a reference density, the model supports phase transitions whenever the control parameter exceeds the critical threshold  $\mathcal{G}_b > \mathcal{G}_b^c$ . In our case,  $\mathcal{G}_b^c = 4$  for an averaged density  $\langle \rho \rangle = \log(2)$ .

We consider  $\mathcal{G}_b$  as an external control parameter, with no need of responding to a self-consistent temperature dynamics. It has been pointed out [30] that the SC model is affected by spurious currents near the interface due to lack of conservation of local momentum. This criticism, however, rests on an ambiguous interpretation of the fluid velocity in the presence of intermolecular interactions. In fact, spurious currents can be shown to disappear completely once the *instantaneous* pre and post-collisional currents are replaced by a time-average over a collisional time. This averaged quantity is readily checked to fulfill both continuity and momentum conservation equations without leading to any spurious current [31]. Let us now consider the main result of this letter, namely the critical interplay between the bulk physics and the presence of wall effects. In fact, in order to make contact with experiments and MD simulations, it is important to include fluid-wall interactions, and notably a parametric form of mesoscopic interactions capable of mimicking wettability properties as described by contact angles between droplets and the solid wall [32]. This effect is achieved by assuming that the interaction with the wall is represented as an external force  $F_w$  normal to the wall and decaying exponentially [28, 29], i.e.

$$F_w(\mathbf{x}) = \mathcal{G}_w \rho(\mathbf{x}) e^{-|\mathbf{x} - \mathbf{x}_w|/\xi} \quad (3)$$

where  $\mathbf{x}_w$  is a vector running along the wall location and  $\xi$  the typical length-scale of the fluid-wall interaction.

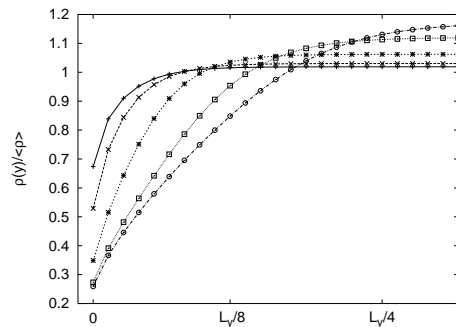


FIG. 1: Rarefaction effects in the full-interaction case  $\mathcal{G}_w, \mathcal{G}_b \neq 0$ . Density profiles are plotted as a function of the distance from the wall, normalized to the channels height ( $y/L_y$ ). The wall interactions have been fixed assuming  $\mathcal{G}_w = 0.03$  and  $\xi = 2$ . The following values of  $\mathcal{G}_b$  are considered:  $\mathcal{G}_b = 1.5$  (+),  $\mathcal{G}_b = 2.5$  (x),  $\mathcal{G}_b = 3.5$  (\*),  $\mathcal{G}_b = 3.9$  (□),  $\mathcal{G}_b = 3.98$  (o). We remind that the bulk phase transition is set at  $\mathcal{G}_b^c = 4$ . In all simulations we choose  $L_y = 80$  grid points for the height of the channel. The volume averaged Knudsen is  $Kn \sim 10^{-3}$ , this would correspond to a channel of a few  $\mu\text{m}$  for liquid water.

Equation (3) has been previously used in literature by using a slightly different LBE scheme to show how the wetting angle depends on the ratio  $\mathcal{G}_w/\mathcal{G}_b$  in presence of phase coexistence between vapor and liquid [28]. Here we want to study the opposite situation, i.e. the effects of  $\mathcal{G}_w$  when the thermodynamically stable bulk physics is governed by a single phase. The main result is that the presence of the wall may trigger a local phase coexistence inducing the formation of a less dense phase in the vicinity of the walls and an apparent slip of the bulk fluid velocity profile extrapolated at the wall location. Equations (1-3) have been numerically solved for different values of the parameters  $\mathcal{G}_b, \mathcal{G}_w$  and  $\xi$  in a two dimensional channel with periodic boundary conditions in the stream-wise  $x$  direction, being  $y = 0$  and  $y = L_y$  the wall positions. The sign of  $\mathcal{G}_w$  is such to give a repulsive force for the liquid particles at the wall.

The flow is driven by a constant pressure gradient in the  $x$  direction  $F_i = \delta_{i,x} \partial_x P_0$ . No-slip boundary conditions are used at the wall and for small Knudsen numbers, i.e. in the large scale limit, the numerical solutions have been checked against its weakly-inhomogeneous macroscopic hydrodynamic limit, namely:

$$\begin{aligned} \partial_t \rho + \partial_i(u_i \rho) &= 0 \\ \rho[\partial_t u_i + (u_j \partial_j)u_i] &= -\partial_i P + \nu \partial_j(\rho \partial_i u_j + \rho \partial_j u_i) + F_i \\ P &= c_s^2 \rho - V_{eff}(\rho) \end{aligned} \quad (4)$$

where subscripts  $i, j$  run over the two spatial dimensions. Above we have  $\nu = c_s^2(\tau - 1/2)$  and  $P$  is the total pressure consisting of an ideal-gas contribution,  $c_s^2 \rho$ , plus the so-called excess pressure,  $V_{eff}$ , due to potential-energy interactions. The expression of  $V_{eff}$  in terms of both  $\mathcal{G}_b$

and  $\mathcal{G}_w$  reads:

$$V_{eff}(\rho) = \frac{1}{2}\mathcal{G}_b(1 - \exp(-\rho))^2 + \mathcal{G}_w \int_0^y ds \rho(s) \exp(-s/\xi).$$

Let us notice that the continuum equation (4) naturally predicts the increase of the mass flow rate in presence of a density profile which becomes more and more rarefied by approaching the wall [18]. Indeed, under stationary conditions, the continuity equation in (4) reduces to  $\partial_y(\rho u_y) = 0$ , which, because of the boundary conditions, implies  $\rho u_y = 0$ , i.e.  $u_y = 0$  everywhere. Thus, in a homogeneous channel along the stream-wise direction, the velocity  $u_x$  satisfies the equation

$$\nu \partial_y(\rho \partial_y u_x) = -\partial_x P_0. \quad (5)$$

In the new variable,  $y' = y - H$ , where  $H = L_y/2$ , we may express the solution of (5) as:

$$u_x(y') = - \int_{y'}^H \frac{s \partial_x P_0}{\nu \rho(s)} ds. \quad (6)$$

Using (6) and assuming that density variations are concentrated in a smaller layer of thickness  $\delta$  near the wall, we can estimate the mass flow rate  $Q_{eff}$  for small  $\delta$  as:

$$\frac{Q_{eff}}{Q_{pois}} = 1 + \frac{3}{2} \frac{\Delta \rho_w}{\rho_w} \frac{\delta}{H} \quad (7)$$

where  $Q_{pois}$  corresponds to the Poiseuille rate  $2\partial_x P_0 H^3/3\nu$  valid for incompressible flows with no-slip boundary conditions. In equation (7), the quantity  $\Delta \rho_w$  is defined as the difference between  $\rho$  computed in the center of the channel and  $\rho_w$  computed at the wall. The effective slip length is then usually defined in terms of the increment in the mass flow rate [17]:

$$\lambda_s \sim \delta \frac{\Delta \rho_w}{\rho_w}. \quad (8)$$

This is the best one can obtain by using a purely continuum approach. The added value of the mesoscopic approach here proposed consists in the possibility to directly compute the density profile, and its dependency on the underlying wall-fluid and fluid-fluid physics. To this purpose, we consider the momentum balance equation in (4) for the direction normal to the wall,  $i = y$ . Since  $u_y = 0$ , we simply obtain  $\partial_y P = 0$ , i.e.

$$c_s^2 \partial_y \rho - 2\mathcal{G}_b(1 - e^{-\rho})e^{-\rho} \partial_y \rho - \mathcal{G}_w \rho e^{-y/\xi} = 0. \quad (9)$$

Let us first study the effects of the wall in (9) by setting  $\mathcal{G}_b = 0$ . One can easily obtain  $\log(\rho(y)/\rho_w) = \frac{\xi \mathcal{G}_w}{c_s^2} (1 - \exp(-y/\xi))$ , which enables us to estimate  $\Delta \rho_w = \rho_w (\exp(\xi \mathcal{G}_w/c_s^2) - 1)$ . Using (8), we obtain for the effective slip-length:

$$\lambda_s \sim \xi e^{\xi \mathcal{G}_w/c_s^2} \quad [\mathcal{G}_b = 0]. \quad (10)$$

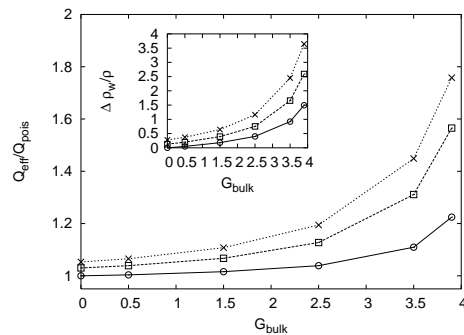


FIG. 2: Increase of the mass flow rate with the coupling strength  $\mathcal{G}_b$  of fluid-fluid bulk interactions. Fixing the wall correlation function  $\xi = 2$ , we plot the mass flow rate ( $Q_{eff}$ ) normalized to its Poiseuille value ( $Q_{pois}$ ) as a function of  $\mathcal{G}_b$  for different values of  $\mathcal{G}_{wall}$ :  $\mathcal{G}_{wall} = 0.0$  ( $\circ$ ),  $\mathcal{G}_{wall} = 0.04$  ( $\square$ ),  $\mathcal{G}_{wall} = 0.08$  ( $\times$ ). Inset: same as the main figure for  $\Delta \rho_w/\rho$ .

We now turn our attention to the non trivial interference between bulk and wall physics whenever  $\mathcal{G}_b > 0$ . Defining the bulk pressure as:  $P_b = c_s^2 \rho - \frac{1}{2}\mathcal{G}_b(1 - \exp(-\rho))^2$ , we can rewrite equation (9) to highlight its physical content as follows:

$$\log\left(\frac{\rho(y)}{\rho_w}\right) = \xi \mathcal{G}_w (1 - e^{-y/\xi}) / \overline{\partial P_b / \partial \rho} \quad (11)$$

where the bulk effects appear only through the following term:

$$\overline{\frac{\partial P_b}{\partial \rho}} \equiv \frac{1}{\log(\rho(y)/\rho_w)} \int_0^y \frac{\partial P_b}{\partial \rho} \frac{d\rho}{\rho}. \quad (12)$$

Equation (11) highlights two results. First, the effect of the bulk can always be interpreted as a renormalization of the wall-fluid interaction by

$$\mathcal{G}_w^R \equiv \mathcal{G}_w / \overline{\frac{\partial P_b}{\partial \rho}}. \quad (13)$$

Second, as it is evident from (13), one must notice that near the bulk critical point where  $\partial P_b / \partial \rho \rightarrow 0$ , the renormalizing effect can become unusually great. In other words, the presence of the wall may locally push the system toward a phase transition even if the bulk physics it is far from the transition point. As a result, the effective slip length in presence of both wall and bulk non-ideal interactions can be estimated as:

$$\lambda_s \sim \xi \exp(\xi \mathcal{G}_w^R) \quad (14)$$

In Fig. 1 we show  $\rho(y)$  for different values of  $\mathcal{G}_b$  and  $\mathcal{G}_w = 0.03$ ,  $\xi = 2$  as obtained by numerically integrating equations (1-3). The numerical simulations have been carried out by keeping fixed the value of  $\langle \rho \rangle = \frac{1}{L_y} \int_0^{L_y} \rho(s) ds = \log(2)$ . As one can see, while  $\mathcal{G}_b \rightarrow \mathcal{G}_c = 4$ , the density difference  $\Delta \rho_w$  between the

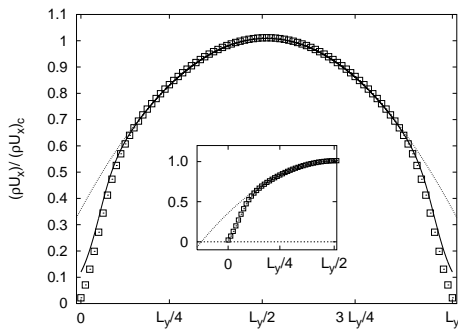


FIG. 3: Momentum profile as a function of the channel height. We plot the momentum profile ( $\rho u_x$ ) normalized to its center channel value ( $(\rho u_x)_c$ ) as a function of the distance from the wall ( $y$ ) normalized to the channel height ( $L_y$ ). The results of numerical simulations ( $\square$ ) with  $\mathcal{G}_b = 3.5$ ,  $\mathcal{G}_w = 0.08$  and  $\xi = 2$  are compared with the analytical estimate (continuous line) obtained solving equations (9) and (6). To highlight the rarefaction effect, the parabolic fit in the center channel region (dotted line) is also plotted. Inset: estimate of the apparent slip length in the channel obtained the same parabolic fit as in the main figure.

center of the channel and the wall increases, as predicted by equation (9). Consequently, the mass flow rate increases as shown in Fig. 2. Let us notice in the same figure that also with  $\mathcal{G}_w = 0$ , the wall initiates a small rarefaction effects due to the fact that fluid particles close to the boundary are attracted only by particles in the bulk of the channel. What we showed here is that the combined actions of  $\mathcal{G}_w$  and  $\mathcal{G}_b \rightarrow \mathcal{G}_b^c$  may strongly increase the formation of this less dense region in the prox-

imity of the surface. For a quantitative check, we have numerically integrated equations (9) and (6) for a given value  $\langle \rho \rangle = \log(2)$ . The analytical estimate for  $\rho u_x$  is compared with the numerical results in Fig. 3. This is a stringent test for our analytical interpretation. The result is that the analytical estimate is able to capture the deviations from a pure parabolic profile at approaching the wall region, where rarefaction effects are present. The crucial point in our analysis is that, even for very small  $\mathcal{G}_w$ , large apparent slip can occur in the channel if  $\mathcal{G}_b$  is close to its critical value, i.e. the limit  $\mathcal{G}_w \rightarrow 0$  and  $\mathcal{G}_b \rightarrow \mathcal{G}_b^c$  do not commute. For example, let us consider the case when  $\mathcal{G}_w \sim \epsilon \ll 1$ ,  $\xi \sim \epsilon$  and  $\mathcal{G}_b \sim \mathcal{G}_b^c - \epsilon^3$ , we obtain  $\frac{\partial P_b}{\partial \rho} \sim \epsilon^3$  and therefore, equation (14) predicts that  $\lambda_s \sim O(1)$  for  $\epsilon \rightarrow 0$ . The wall effect, parametrized by  $\mathcal{G}_w$  and  $\xi$ , can act as a catalyzer in producing large apparent slip. Most of the results shown in Figs. (1) and (2) are in close agreement with the MD numerical simulations [4, 5, 7, 8]. Our analysis points out that, close to the wall, one can observe a “local phase transition” triggered by the presence of the wall itself. In summary, we have shown that a suitable form of the Lattice Boltzmann Equation can be proposed in order to simulate apparent slip in microchannel. Slip boundary conditions arise spontaneously because, close to the wall, a “gas” layer is formed. If the system is close to a state where coexistence of different phases (liquid and gas) are thermodynamically achievable, then, macroscopic slip effects can result. We have shown that for large scale separation, the model reduces to a continuum set of hydrodynamical equations which explains the qualitative and quantitative behavior of the mass flow rate in terms of the model parameters, i.e.  $\mathcal{G}_b$  and  $\mathcal{G}_w$ .

- 
- [1] B. Massey, *Mechanics of Fluids* (Chapman and Hall, 1989).
- [2] C.-M. Ho and Y.-C. Tai, *Annu. Rev. Fluid Mech.* **30** 579 (1998).
- [3] P. Tabeling, *Introduction á la microfluidique* (Belin, 2003).
- [4] J.-L. Barrat and L. Bocquet, *Phys. Rev. Lett.* **82** 4671 (1999).
- [5] M. Cieplak, J. Koplik and J.R. Banavar, *Phys. Rev. Lett.* **86** 803 (2001).
- [6] P. Thompson and S.M. Troian, *Nature* **389** 360 (1997).
- [7] A.A. Darhuber and S.M. Troian, *Ann. Rev. Fluid Mech.* **37** 425 (2005).
- [8] C. Cottin-Bizonne, C. Barentin, E. Charlaix et al. *Europ. Phys. Journ. E* **15** 427 (2004).
- [9] D. Y. C. Chan and R. G. Horn, *J. Chem. Phys.* **83** 5311(1985).
- [10] J. N. Israelachvili, P. M. McGuiggan and A. M. Homola, *Science* **240** 189 (1988).
- [11] J. Klein and E. Kumacheva, *Science* **269** 816 (1995).
- [12] U. Raviv, P. Laurat and J. Klein, *Nature* **413** 51 (2001).
- [13] C. Choi, K. Johan, A. Westin and K. Breuer, *Phys. of Fluids* **15** 2897 (2003).
- [14] J.-T. Cheng and N. Giordano, *Phys. Rev. E* **65** 031206 (2002).
- [15] R. Pit, H. Hervet and L. Leger, *Phys. Rev. Lett.* **85** 980 (2000).
- [16] P. Joseph and P. Tabeling *Phys. Rev. E* **71**, 035303(R) (2005).
- [17] E. Lauga, M.P. Brenner, H.A. Stone, “The no-slip boundary condition: a review” cond-mat/0501557.
- [18] D. Tretheway and C. Meinhart, *Phys. Fluids* **16** 1509 (2004).
- [19] P. G. de Gennes, *Langmuir* **18** 3413 (2002).
- [20] S. Succi, *The lattice Boltzmann Equation* (Oxford Science, 2001).
- [21] D. Wolf-Gladrow, *Lattice-Gas Cellular Automata and Lattice Boltzmann Models* (Springer, 2000).
- [22] X. Shan and H. Chen, *Phys. Rev. E* **47** 1815 (1993); *Phys. Rev. E* **49** 2941 (1994).
- [23] R. Benzi, S. Succi, M. Vergassola, *Phys. Rep.* **222** 145 (1992).
- [24] M.R. Swift, W.R. Osborn and J.M. Yeomans, *Phys. Rev. Lett.* **75** 830 (1995).

- [25] R. Verberg and A.J.C. Ladd, *Phys Rev. Lett.* **84** 2148 (2000).
- [26] R. Verberg, C.M. Pooley, J.M. Yeomans and A.C. Balazs, *Phys. Rev. Lett.* **93** 1845011 (2003).
- [27] D. Kwok, *Phys. Rev. Lett.* **90** 1245021 (2003).
- [28] J. Zhang and D. Kwok, *Phys. Rev. E* **70** 056701 (2004);  
J. Zhang B. Ling and D. Kwok, *Phys. Rev. E* **69** 032602 (2004).
- [29] D.E. Sullivan, *J. Chem. Phys.* **74** 2604 (1981).
- [30] R.R. Nourgaliev, T.N. Dinh, T.G. Theofanous and D. Joseph, *Int. Jour. of Multiphase Flow* **29** 117 (2003).
- [31] J.M. Buick and C.A. Greated, *Phys. Rev. E* **61** 5307 (2000).
- [32] P. G. de Gennes, *Rev. Mod. Phys.* **3** 827 (1985).